Generalized coherent states for the Pöschl-Teller potential and a classical limit

M. G. A. Crawford and E. R. Vrscay
Department of Applied Mathematics, University of Waterloo, Waterloo, Ontario, Canada N2L 3G1

(Received 22 August 1997)

Coherent states in the harmonic oscillator may be defined in several equivalent ways. One definition describes coherent states as special states satisfying a minimum-uncertainty requirement in position and momentum spaces. This definition is generalized for other potentials according to a method developed by Nieto *et al.* [Phys. Rev. D **20**, 1321 (1979)] and is herein applied to the Pöschl-Teller potential. A classical limit based on the harmonic-oscillator coherent-state classical limit is then developed and applied to the Pöschl-Teller minimum-uncertainty states. In this limit, classical behavior may be obtained from these quantum states. Together with a completeness argument for the generalized coherent states, this result provides insight into quantum classical correspondence through the statistical interpretation of quantum mechanics.
[S1050-2947(98)05001-X]

PACS number(s): 03.65.−w, 03.65.Ca, 02.90.+p

I. INTRODUCTION

Coherent states were first introduced to quantum mechanics by Schrödinger in 1926 [1], who immediately envisioned them as some kind of intermediate step between quantum and classical mechanics. The appealing properties of these states include minimum uncertainty, an infinite coherence time, and expectation values that follow classical trajectories in time. These states can also be shown to form a complete set of states.

Unfortunately, the important properties of these states, particularly those involving time evolution, are valid only in the harmonic-oscillator case. Accordingly, much effort has been put into generalizing these states for other potentials; the physically interesting hydrogen atom problem appears to have been the most frequent subject [2,3]. Unlike most generalizations that target specific potentials, we consider the generalization due to Nieto [4–9], who have provided a broadly applicable algorithm for the definition of minimum-uncertainty coherent states (MUCSs).

II. GENERALIZED COHERENT STATES

Indeed, much has been written about harmonic-oscillator coherent states (HOCSs) [10]. For purposes of reference and comparison, some of the central results are summarized in the Appendix.

A. Nieto's generalization of coherent states

Coherent states for the harmonic oscillator give the motivation for defining coherent states in other potentials. Due to the special characteristics of the harmonic oscillator, however, generalizations for ''less ideal'' potentials will likely not behave so well, implying in turn that states are not expected to cohere for all time. Thus the thrust of Nieto's generalization of MUCSs, outlined below, is to define states that cohere and follow classical trajectories for the longest possible time. For a complete description of the generalization, the reader should consult the original papers [4–9].

Suppose $V(x)$ is a potential with only one minimum. Classical trajectories in this potential will follow simple closed orbits in x-p phase space. There exists a one-to-one map from this orbit to an elliptical orbit in transformed coordinates, X_c and $P_c = m\dot{X}_c$, which is an ellipse so that X_c and P_c vary sinusoidally with time. Note that P_c is *not* the momentum conjugate to X_c. To find X_c, solve the differential equation

$$\frac{d}{dx}X_c = \omega\left(\frac{m(A^2 - X_c^2)}{2[E - V(x)]}\right)^{1/2} \tag{1}$$

and make a choice for the arbitrary constant. Coordinates in which orbits are ellipses are thought of as the ''natural'' coordinates of the system.

Now define the quantum operators

$$\hat{X} = X_c(\hat{x}) \tag{2}$$

and

$$\hat{P} = \frac{1}{2}[X_c'(\hat{x})\hat{p} + \hat{p}X_c'(\hat{x})]. \tag{3}$$

This is done so that the general potential has the form of the harmonic oscillator through the new operators $\hat{X}$ and $\hat{P}$. In the quantum system, the inner products $\langle\phi_m|\hat{X}|\phi_n\rangle$ and $\langle\phi_m|\hat{P}|\phi_n\rangle$ are nonzero only for $n = m \pm 1$, as for $\hat{x}$ and $\hat{p}$ in the harmonic oscillator. These properties make $\hat{X}$ and $\hat{P}$ the natural operators to employ for a given potential.

A third operator $\hat{G}$ is now defined according to the commutator

$$\hat{G} = -i[\hat{X},\hat{P}] = \hbar[X_c'(\hat{x})]^2. \tag{4}$$

As with the untransformed $\hat{x}$ and $\hat{p}$,

$$(\Delta X)^2(\Delta P)^2 \leqslant \frac{1}{4}\langle G\rangle^2. \tag{5}$$

Minimum-uncertainty coherent states that satisfy the equality in Eq. (5) will be solutions of the problem

$$\frac{1}{2}\left(\frac{\hat{X}}{\Delta X}+\frac{i\hat{P}}{\Delta P}\right)|\psi\rangle=\alpha|\psi\rangle,$$
$$\alpha=\frac{1}{2}\left(\frac{\langle X\rangle}{\Delta X}+\frac{i\langle P\rangle}{\Delta P}\right). \tag{6}$$

The coherent state is defined by α, which depends on four parameters, one of which is eliminated by the equality in Eq. (5) and another by the requirement that the ground state be recovered by $\alpha=0$. If the algorithm is applied to the harmonic oscillator, it is simple to demonstrate that the HOCSs are regained.

B. The Pöschl-Teller potential

Following Nieto and Simmons [5] the algorithm is applied to the one-dimensional Pöschl-Teller potential, with the associated Hamiltonian ($\lambda>1$)

$$\hat{H}=\frac{\hat{p}^2}{2m}+V(\hat{x}), \quad V(x)=U_0\tan^2 ax,$$
$$U_0=\frac{\hbar^2 a^2}{2m}\lambda(\lambda-1). \tag{7}$$

The eigenenergies of this Hamiltonian are given by [11]

$$E_n=\frac{\hbar^2a^2}{2m}(n^2+2n\lambda+\lambda), \quad n=0,1,2,\ldots, \tag{8}$$

and corresponding eigenstates by

$$\langle x|\phi_n\rangle=N_n\cos^{1/2}ax \ \ P^{1/2-\lambda}_{n+\lambda-1/2}(\sin ax), \tag{9}$$

where

$$N_n=\left(\frac{a(n+\lambda)\Gamma(n+2\lambda)}{\Gamma(n+1)}\right)^{1/2}, \tag{10}$$

and the $P^{\nu}_{\mu}(y)$ are the associated Legendre functions.

Classical motion in the Pöschl-Teller potential is given by

$$x(t)=\frac{1}{a}\arcsin[A\sin(\omega t+\phi)], \tag{11}$$

where

$$A=\sqrt{\frac{E}{E+U_0}}, \quad \omega=a\sqrt{\frac{2}{m}(E+U_0)}, \tag{12}$$

E is the total energy, and the constant ϕ is chosen to match initial conditions. Given Eq. (11), it is not difficult to obtain that

$$X_c(x)=\sin ax \tag{13}$$

would render sinusoidal trajectories. In the general case, one would have to solve the differential equation (1) to find X_c.

Using the transformation (13) we define the quantum operators $\hat{X}$ and $\hat{P}$ according to Eqs. (2) and (3),

$$\hat{X}=\sin a\hat{x}, \quad \hat{P}=\frac{a}{2}(\cos a\hat{x} \ \ \hat{p}+\hat{p}\cos a\hat{x}), \tag{14}$$

and calculate their commutator

$$\hat{G}=-i[\hat{X},\hat{P}]=\hbar a^2\cos^2 a\hat{x}, \tag{15}$$

so that the MUCSs developed by this algorithm satisfy the equality in the uncertainty relation

$$(\Delta X)^2(\Delta P)^2\geqslant\frac{1}{4}\langle\hbar a^2\cos^2 ax\rangle^2. \tag{16}$$

From Eq. (6), the coherent states are solutions of

$$\frac{1}{2}\left(\frac{\sin a\hat{x}}{\Delta X}+\frac{ia}{2}\,\frac{\cos a\hat{x} \ \ \hat{p}+\hat{p}\cos a\hat{x}}{\Delta P}\right)|\psi\rangle=\alpha|\psi\rangle, \tag{17}$$

where

$$\alpha=\frac{1}{2}\left(\frac{\langle X\rangle}{\Delta X}+i\frac{\langle P\rangle}{\Delta P}\right). \tag{18}$$

Taking the inner product of Eq. (17) with $\langle x|$, we obtain a first-order differential equation with the solution

$$\langle x|\psi_{MUS}\rangle=N_{MUS}(\cos ax)^B\left(\frac{1+\sin ax}{1-\sin ax}\right)^{C/2}, \tag{19}$$

with

$$B=\frac{\Delta P}{a^2\hbar\Delta X}-\frac{1}{2}, \quad C=\frac{2\alpha\Delta P}{a^2\hbar}=u+iv, \tag{20}$$

and

$$N_{MUS}=\left(\frac{a}{\sqrt{\pi}}\,\frac{\Gamma\left(B+\frac{1}{2}\right)\Gamma(B+1)}{\Gamma\left(B-u+\frac{1}{2}\right)\Gamma\left(B+u+\frac{1}{2}\right)}\right)^{1/2}. \tag{21}$$

The ground state for the Pöschl-Teller potential is given by

$$\langle x|\phi_0\rangle=\left(\frac{a}{\sqrt{\pi}}\,\frac{\Gamma(\lambda+1)}{\Gamma\left(\lambda+\frac{1}{2}\right)}\right)^{1/2}(\cos ax)^{\lambda}. \tag{22}$$

When $\alpha=0$, $C=0$ and the coherent state (19) becomes

$$\langle x|\psi_{MUS}\rangle=\left(\frac{a}{\sqrt{\pi}}\,\frac{\Gamma(B+1)}{\Gamma\left(B+\frac{1}{2}\right)}\right)^{1/2}(\cos ax)^B, \tag{23}$$

so that $B=\lambda$. From Eq. (20),

$$\frac{\Delta P}{\Delta X}=a^2\hbar\left(\lambda+\frac{1}{2}\right) \tag{24}$$

and the variation of C defines a family of MUCSs that contains the ground state.

The quantity $\langle\cos^2 ax\rangle^2$ on the right-hand side of Eq. (16) can be calculated to yield

$$\langle\cos^2 ax\rangle = \frac{\left(\lambda+\frac{1}{2}\right)^2 - u^2}{(\lambda+1)\left(\lambda+\frac{1}{2}\right)}. \tag{25}$$

Combining Eqs. (25), (16), and (24), the uncertainties in $\hat{X}$ and $\hat{P}$ become

$$(\Delta X)^2 = \frac{1}{2}\,\frac{\left(\lambda+\frac{1}{2}\right)^2 - u^2}{(\lambda+1)\left(\lambda+\frac{1}{2}\right)^2} \tag{26}$$

and

$$(\Delta P)^2 = \frac{1}{2}\hbar^2 a^4 \frac{\left(\lambda+\frac{1}{2}\right)^2 - u^2}{\lambda+1}. \tag{27}$$

This sheds some additional light on the parameter of the coherent state $C = u + iv$, which is, from Eq. (20),

$$C = \alpha\left(\frac{\left(\lambda+\frac{1}{2}\right) - u^2}{2a^2(\lambda+1)}\right)^{1/2}. \tag{28}$$

From Eqs. (20) and (18) we have

$$\langle X\rangle = \frac{u}{\lambda+\frac{1}{2}}, \quad \langle P\rangle = \hbar a^2 v. \tag{29}$$

The expectation value of the Hamiltonian can also be calculated to be

$$\langle H\rangle = \frac{\hbar^2 a^2}{2m}\left(\frac{\lambda\left(\lambda-\frac{1}{2}\right)}{\left(\lambda-\frac{1}{2}\right)^2 - u^2}(u^2+v^2) + \lambda\right). \tag{30}$$

It is convenient to express these coherent states as a superposition of the Pöschl-Teller eigenstates (9). The expansion coefficients a_n are given, after extensive calculations, by

$$a_n = \frac{2^{\lambda+1/2}\Gamma\left(-\frac{C}{2}+\lambda+\frac{1}{2}\right)}{\pi^{1/4}\Gamma\left(\lambda+\frac{3}{2}\right)}\left(\frac{\Gamma(\lambda+1)}{\Gamma\left(\lambda+\frac{1}{2}\right)\Gamma\left(\lambda+\frac{1}{2}+u\right)\Gamma\left(\lambda+\frac{1}{2}-u\right)}\right)^{1/2}$$
$$\times\left(\frac{(\lambda+n)\Gamma(2\lambda+n)}{\Gamma(n+1)}\right)^{1/2} {}_3F_2\left(\begin{matrix} -n-\lambda+\frac{1}{2}, n+\lambda+\frac{1}{2}, -\frac{C}{2}+\lambda+\frac{1}{2}; \\ \lambda+\frac{1}{2}, \quad \lambda+\frac{3}{2}; \end{matrix}\; 1\right). \tag{31}$$

Note that the expansion given by Nieto and Simmons [5] appears to be incorrect: Their calculation employs a representation of associated Legendre functions in terms of hypergeometric functions [see [12], Eq. (8.772.3)] that is valid over only the positive half of the potential. However, their expansion was not ever used in their calculations. The expansion (31) was employed in this study.

III. CLASSICAL LIMITS OF COHERENT STATES

A. The harmonic-oscillator coherent-state classical limit

The classical limit for harmonic-oscillator coherent states involving large values of the parameter $|\alpha|$ [of Eq. (A4)] and the smallness of $\hbar$ has been around for a long time [13]. Bhaumik and Dutta-Roy [14] employed a limit $\hbar\to 0$, $|\alpha|\to\infty$ with $A = 2|\alpha|\sqrt{\hbar/2m\omega}$ fixed to construct perturbed coherent states for anharmonic oscillators. This coherent-state perturbation method and its classical limit was further analyzed by Benoit, McRae, and Vrscay [15] and by McRae and Vrscay [16]. In the latter study, a connection was made between the Bhaumik–Dutta-Roy procedure and classical limit of eigenstates of Rayleigh-Schrödinger perturbation expansions in which the classical action J is fixed (i.e., $n\to\infty$, $\hbar\to 0$ while $J = n\hbar$ is fixed). As a result, their classical limit of coherent states involved $\hbar\to 0$, $|\alpha|\to\infty$ with $J = |\alpha|^2\hbar$ fixed. In all cases, the limit produces a state that behaves as a single classical trajectory. It was also shown explicitly how an action-preserving classical limit of the harmonic oscillator coherent-state expansion in Eq. (A4) yields an ensemble of classical trajectories that produce the classical distribution.

We also insert the usual disclaimer that the operation "$\hbar\to 0$" does not involve the adjustment of a physical constant, but rather an account of the size of the constant $\hbar$ as compared to the "characteristic action" of the system. Accordingly, for the descriptions of these limits, define $\eta = \hbar/\kappa$, where κ is the characteristic action of the system. The remainder of this paper is concerned with the limiting behavior when $\eta\to 0$.

The harmonic-oscillator coherent state has an expectation value of energy equal to

$$\langle H\rangle=\frac{\langle p^2\rangle}{2m}+\frac{1}{2}m\omega^2\langle x^2\rangle=\eta\omega\left(|\alpha|^2+\frac{1}{2}\right). \tag{32}$$

From Eqs. (A12) and (A13), the amplitude of the oscillations in position and momentum space is given by

$$A^2=\langle x\rangle^2+\frac{\langle p\rangle^2}{m^2\omega^2},\quad B^2=\langle p\rangle^2+m^2\omega^2\langle x\rangle^2. \tag{33}$$

The angular frequency of these oscillations is ω.

With a HOCS, we associate a classical trajectory with $x_0=\langle x\rangle$ and $p_0=\langle p\rangle$. Its energy is given by

$$E=\frac{p_0^2}{2m}+\frac{1}{2}m\omega^2x_0^2 \tag{34}$$

and the amplitudes in x and p are

$$A_c^2=x_0^2+\frac{p_0^2}{m^2\omega^2},\quad B_c^2=p_0^2+m^2\omega^2x_0^2. \tag{35}$$

Once again, the angular frequency of oscillation is ω. Thus the expectation value of the quantum wave function follows the classical trajectory with the same initial conditions, with the exception of the energy, which, in the quantum state, is $\frac{1}{2}\eta\omega$ larger than for the classical particle.

The premise of the classical limit of the HOCS is to let $\eta\to 0$ or $\nu\to\infty$, while fixing the action J_c of the associated classical trajectory. From Eq. (35),

$$J_c=\pi\left(m\omega x_0^2+\frac{p_0^2}{m\omega}\right)=2\pi\eta|\alpha|^2, \tag{36}$$

so that the goal is accomplished through fixing $J=\eta|\alpha|^2$ while sending $\eta\to 0$. Then, from Eqs. (A9), (A10), and (32), $\Delta x\to 0$, $\Delta p\to 0$, and $\langle H\rangle\to E$; the limiting state describes exactly a single classical trajectory in terms of a distribution.

B. The classical limit of Nieto's generalized coherent states

The crucial points to preserve in the generalization of the harmonic-oscillator coherent-state classical limit are $|\alpha|\to\infty$ and the fixed action J_c of the associated classical trajectory. Recall as well the use of the effective Planck constant η.

The coherent states, in addition to satisfying the equality in Eq. (5), have a fixed ratio ΔX to ΔP, or

$$\frac{\Delta X}{\Delta P}=K, \tag{37}$$

for some constant K. Hence

$$(\Delta X)^2=\frac{\eta}{2}K\langle[X_c'(x)]^2\rangle \tag{38}$$

and

$$(\Delta P)^2=\frac{\eta}{2}\frac{\langle[X_c'(x)]^2\rangle}{K}. \tag{39}$$

Substituting these into the expression for α, Eq. (6) becomes

$$\alpha=\frac{1}{\sqrt{2\eta K\langle[X_c'(x)]^2\rangle}}[\langle X\rangle+iK\langle P\rangle]. \tag{40}$$

The expectation values $\langle X\rangle$ and $\langle P\rangle$ remain small as $|\alpha|$ becomes large since the classical action J_c is fixed. Therefore, $\eta\to 0$, which implies that $\Delta X\to 0$ and $\Delta P\to 0$ as well. Since the right-hand side of Eq. (1) is positive, $X_c(x)$ is monotonically increasing in x, as is P_c with p. Hence, as $\Delta X\to 0$ and $\Delta P\to 0$, then $\Delta x\to 0$ and $\Delta p\to 0$ as well. With the uncertainties going to zero, the distributions become δ functions in both position and momentum spaces.

C. The Pöschl-Teller analog

Note that the Pöschl-Teller potential, unlike the harmonic oscillator, is defined in terms of $\hbar$ (or rather η). The classical limit involves $\eta\to 0$, so we must explicitly preserve the shape of the potential by fixing U_0. Examining Eq. (7), we anticipate that this involves λ becoming large as η becomes small.

The first aspect of the classical limit to examine is the dependence of the action of the classical trajectory on α. From Eq. (7),

$$p(x)=\sqrt{2m(E-U_0\tan^2 ax)}. \tag{41}$$

The classical turning points $\pm x_0$ are given by

$$x_0=\frac{1}{a}\arctan\sqrt{\frac{E}{U_0}}, \tag{42}$$

so that

$$\begin{aligned}J_c&=2\int_{-x_0}^{x_0}\sqrt{2m(E-U_0\tan^2 ax)}dx\\&=\frac{\pi}{a}\sqrt{\frac{m}{2}}(\sqrt{E+U_0}-\sqrt{U_0}).\end{aligned} \tag{43}$$

Hence J_c is fixed if and only if the energy of the associated classical trajectory E is held fixed. The energy E is given by

$$E=\frac{p_0^2}{2m}+U_0\tan^2 ax_0, \tag{44}$$

in which x_0 and p_0 are given by the initial expectation values of the position and momentum in the coherent state. Note that we are at liberty to simply choose $\langle X\rangle=\langle x\rangle=x_0=0$, so that to vary $|\alpha|$ is to change only $\langle P\rangle$ and $\langle p\rangle=p_0$. From Eq. (29), $u=0$. Recall that $C=u+iv$ so that, after some calculation,

$$\langle p\rangle=\eta av\frac{\lambda\Gamma(\lambda)^2}{\Gamma(\lambda+\frac{1}{2})^2}=\frac{\eta\,\mathrm{Im}(\alpha)}{\sqrt{2}}\frac{\lambda\Gamma(\lambda)^2}{\Gamma(\lambda+\frac{1}{2})^2}\left(\frac{\lambda+\frac{1}{2}}{\lambda+1}\right)^{1/2}. \tag{45}$$

Now, given an initial λ_0 defining the potential, U_0 is fixed by keeping

TABLE I. Parameters of calculations in the Pöschl-Teller limit. The quantities ω and T are the classical frequency and period, respectively. In all cases, $U_0=4.3750$. Column 1 lists curves in Fig. 2.

Curve	λ	$\hbar$	ν	$\langle H\rangle$	ω	T
(a)	$\frac{7}{2}$	1	5	14.58	6.1577	1.0204
(b)	$\frac{15}{2}$	4.236×10^{-1}	1.180×10^{1}	13.39	5.9612	1.0540
	$\frac{31}{2}$	1.973×10^{-1}	2.534×10^{1}	12.91	5.8808	1.0684
(c)	$\frac{63}{2}$	9.543×10^{-2}	5.239×10^{1}	12.70	5.8441	1.0751
	$\frac{127}{2}$	4.695×10^{-2}	1.064×10^{2}	12.59	5.8265	1.0784
(d)	$\frac{255}{2}$	2.329×10^{-2}	2.146×10^{2}	12.54	5.8179	1.0800
	$\frac{511}{2}$	1.160×10^{-2}	4.310×10^{2}	12.52	5.8137	1.0808
(e)	$\frac{1023}{2}$	5.788×10^{-3}	8.637×10^{2}	12.51	5.8116	1.0811

$$U=\eta^2\lambda(\lambda-1)=\hbar^2\lambda_0(\lambda_0-1) \tag{46}$$

constant. This is accomplished by setting

$$\lambda=\frac{1}{2}+\sqrt{\frac{1}{4}+\frac{U\nu^2}{\hbar^2}}=\frac{1}{2}+\sqrt{\frac{1}{4}+A\nu^2}, \tag{47}$$

where A is constant, so that λ becomes large as ν grows.

Finally, to fix the action of the associated classical trajectory, we fix the quantity $J=\eta|\alpha|$. (Compare with $J=\eta|\alpha|^2$ for the harmonic oscillator.) To justify this, we observe that the portion in Eq. (45) dependent on λ is reasonably approximated by 1,

$$\frac{\lambda\Gamma(\lambda)^2}{\Gamma(\lambda+\frac{1}{2})^2}\left(\frac{\lambda+\frac{1}{2}}{\lambda+1}\right)^{1/2}=1+\frac{3}{16\lambda^2}+O(\lambda^{-3}), \tag{48}$$

as $\lambda\to\infty$ Thus, fixing $J=\eta|\alpha|$ fixes (to within a reasonable approximation) $\langle p\rangle$, E, and J_c in succession.

In this limit, the uncertainties in X and P become

$$\lim_{\nu\to\infty}(\Delta X)^2=\lim_{\nu\to\infty}\frac{1}{3+\sqrt{1+4A\nu^2}}=0 \tag{49}$$

and

$$\lim_{\nu\to\infty}(\Delta P)^2=\lim_{\nu\to\infty}\frac{\hbar_0^2a^2}{\nu^2}\frac{\left(1+\sqrt{\frac{1}{4}+A\nu^2}\right)^2}{3+\sqrt{1+4A\nu^2}}=0, \tag{50}$$

implying that the transformed position and momentum distributions become δ-function distributions. The operator $\hat{X}=\sin a\hat{x}$ is one to one and monotonic in $\hat{x}$ on $x\in[-\pi/2a,\pi/2a]$. It follows that $(\Delta X)^2\to0$ implies that $(\Delta x)^2\to0$. Similarly, $(\Delta p)^2\to0$, so that the untransformed distributions are also δ functions.

D. The time evolution of Pöschl-Teller coherent states

The only practical way to study the time evolution of these states is through numerical means. To do this, we calculate the eigenfunction expansion using Eq. (31). The time evolution is then obtained by evolving each of the eigenstates individually.

A summary of our numerical results is given in Table I. The time evolution of one such state is shown in Fig. 1.

The distance between expectation values and classical trajectories is determined using

$$d_1(x(t),\langle x(t)\rangle)=\sqrt{\left(\frac{x(t)-\langle x(t)\rangle}{A}\right)^2+\left(\frac{p(t)-\langle p(t)\rangle}{B}\right)^2}, \tag{51}$$

from which we calculate

$$d(x(t),\langle x(t)\rangle)=\frac{1}{t}\int_0^t d_1(x(s),\langle x(s)\rangle)ds, \tag{52}$$

where $A=|x(t)|$ and $B=|p(t)|$ are the position and momentum amplitudes of the classical trajectory, respectively. Note that if the measure d is applied to coherent states in the harmonic oscillator, $d(t)=0$ for all t. The numerical values of this measure are shown in Fig. 2. Note that these measures oscillate with a dominant frequency twice that of the frequency of the classical trajectory: The quantum wave packet has difficulty moving all the way out to the classical turning point.

The simplest way to designate when the quantum and classical trajectories no longer follow one another is to ascertain when the distance d between the classical and quantum trajectories exceeds a certain threshold quantity. A threshold quantity of 0.25 was chosen and the times at which d exceeds this threshold are recorded in Fig. 3. In Fig. 3(b), the interval of agreement is shown to be proportional to $1/\sqrt{\eta}$. An interesting observation is that if we let $a=1\ \mathrm{m}^{-1}$ and $m=1$ kg, then the associated classical system has a 1 kg mass in a potential about 3 m wide. With U_0 set the same as in this sequence of states and $\eta=\hbar$ at its true value of 1.0546×10^{-34} J s, then if this trend continues, the quantum state would evolve close to the classical state for about 4×10^9 years, according to the measure d. Although this is less than the age of the universe, it is rather long and indeed involves about 10^{17} periods of oscillation.

As a strictly numerical consideration, λ values were chosen to be half integral so as to terminate the hypergeometric series in Eq. (31) and to provide associated Legendre functions of integer order and series. We are at liberty to do this because as long as $J=\eta|\alpha|$ and Eq. (47) are satisfied, it does not matter in which order the parameters are chosen.

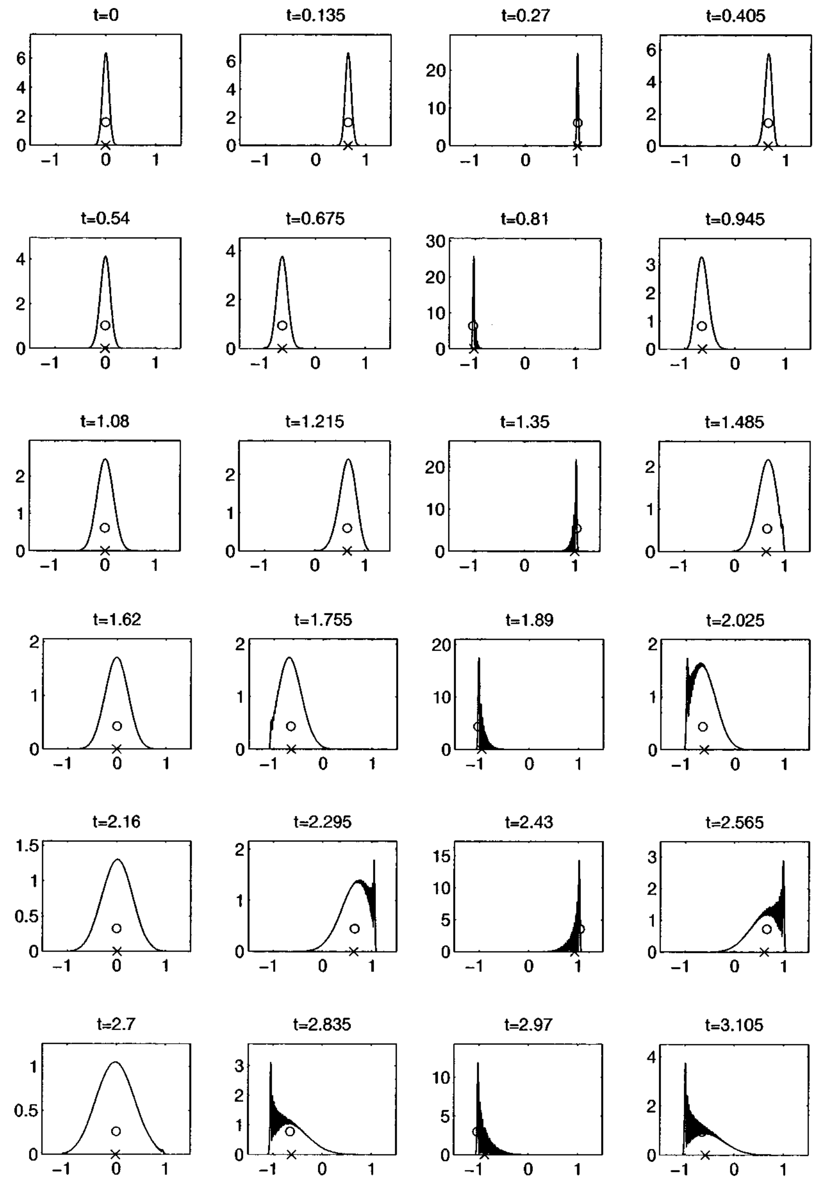

FIG. 1. Time evolution of $|\langle x|\psi\rangle|^2$ plotted vs position x for a MUCS in the Pöschl-Teller potential. The quantum $\langle x\rangle$ is given by the $\times$ at the bottom of each frame and the classical $x(t)$ by the circle.

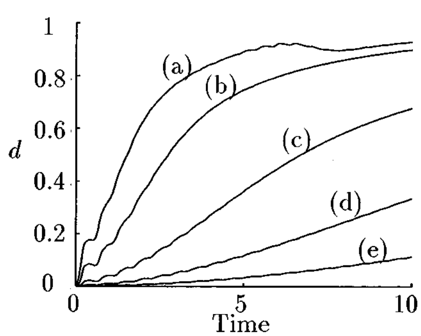

FIG. 2. Distance between $\langle x(t)\rangle$ and $x(t)$ measured according to the measure d. Curves labeled $(a)-(e)$ correspond to entries in Table I.

IV. CONCLUDING REMARKS

The results of the numerical experiments are in agreement with Ehrenfest's theorem according to which expectation values evolve classically provided uncertainties in the posi-

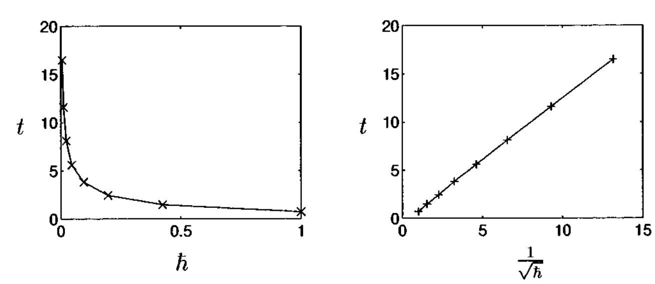

FIG. 3. Time at which $d(x(t),\langle x(t)\rangle)$ exceeds 0.25 vs (a) $\hbar$ and (b) $\hbar^{-1/2}$.

tion and momentum are small. A great deal of caution must be employed when interpreting the implications of this theorem. As observed by Ballentine *et al.* [17], it is untrue that the difference between quantum systems and classical systems arises from these uncertainties. Employing the Liouville equation, one can derive almost identical equations governing the time evolution of classical distributions. However, this does not deny that expectation values for distributions in position and momentum space approaching δ-function distributions follow classical trajectories.

Thus, with $(\Delta x)^2$ becoming small in our limit, the expectation values of our coherent state begin to behave classically. Of course, this estimate of $(\Delta x)^2$ is only valid at $t=0$, so we can only say that the initial behavior of the trajectories will be classical. However, as η (the effective Planck constant) becomes smaller, uncertainties remain small for longer periods of time, resulting in longer intervals of classical behavior.

Indeed, using the standard expression for the time evolution of expectation values,

$$\frac{d}{dt}\langle O\rangle = \frac{i}{\eta}\langle \psi(t)|[\hat{H},\hat{O}]|\psi(t)\rangle + \left\langle \psi(t)\left|\frac{\partial \hat{O}}{\partial t}\right|\psi(t)\right\rangle, \tag{53}$$

and the definitions $\delta\hat{x}=\hat{x}-\langle x\rangle$ and $\delta\hat{p}=\hat{p}-\langle p\rangle$, it is easily shown that

$$\frac{d}{dt}(\Delta x)^2 = \frac{d}{dt}\langle(\delta\hat{x})^2\rangle = \frac{1}{m}\langle \delta\hat{x}\,\delta\hat{p} + \delta\hat{p}\,\delta\hat{x}\rangle. \tag{54}$$

From Eqs. (26), (27), and (47) we have

$$(\Delta x)^2 = \langle(\delta\hat{x})^2\rangle = O(\eta) \ \text{ as } \eta\to 0 \tag{55}$$

and

$$(\Delta p)^2 = \langle(\delta\hat{p})^2\rangle = O(\eta) \ \text{ as } \eta\to 0. \tag{56}$$

Applying these results to Eq. (54) eventually gives

$$\frac{d}{dt}(\Delta x) = O(\eta^{1/2}). \tag{57}$$

Suppose that the rate of change in the uncertainty is roughly constant. Also suppose that when the uncertainty exceeds a certain value, the quantum coherent state fails to follow a classical trajectory. From a linearization of Eq. (57), the length of time Δt that it takes for the uncertainty in position to exceed a certain value behaves according to

$$\Delta t = O(\eta^{-1/2}) \ \text{ as } \eta\to 0. \tag{58}$$

This is demonstrated in Fig. 3(b).

In conclusion, the standard HOCS classical limit has been generalized and applied to Nieto's generalization of the MUCSs. This generalization involves taking $|\alpha|\to\infty$ while fixing the action of the associated classical trajectory. In order to do this, it is necessary for the ''effective Planck's constant'' η to go to zero according to some power law with $|\alpha|$. This algorithm was applied to the Pöschl-Teller MUCSs and the result was a sequence of states that converges to the classical case in the limit.

ACKNOWLEDGMENTS

The authors are grateful to the Natural Sciences Engineering Research Council of Canada (M.G.A.C.) for financial support and an Operating Grant in Aid of Research (E.R.V.).

APPENDIX: HARMONIC-OSCILLATOR COHERENT STATES

The one-dimensional harmonic-oscillator Hamiltonian is given by

$$\hat{H} = \frac{\hat{p}^2}{2m} + \frac{1}{2}m\omega^2\hat{x}^2, \tag{A1}$$

with eigenstates

$$\langle x|n\rangle = \left(\frac{a_0}{\sqrt{\pi}2^n n!}\right)^{1/2}\exp\left(-\frac{1}{2}a_0^2x^2\right)H_n(a_0x), \tag{A2}$$

where $a_0^2=m\omega/\hbar$ and the $H_n(y)$ are the Hermite polynomials of order n. The corresponding eigenenergies are given by

$$E_n = \hbar\omega\left(n+\frac{1}{2}\right), \quad n=0,1,2,\ldots. \tag{A3}$$

The HOCSs are given by

$$|\alpha\rangle = \exp\left(-\frac{|\alpha|^2}{2}\right)\sum_{n=0}^{\infty}\frac{\alpha^n}{\sqrt{n!}}|n\rangle, \tag{A4}$$

where α is a complex parameter. In the coherent state,

$$\langle x\rangle = 2\Delta x\ \mathrm{Re}(\alpha), \quad \langle p\rangle = 2\Delta p\ \mathrm{Im}(\alpha). \tag{A5}$$

Using the Gaussian as the generating function for the Hermite polynomials, it is not difficult to show

$$\langle x|\alpha\rangle = \left(\frac{1}{2\pi(\Delta x)^2}\right)^{1/4}\exp\left[-\left(\frac{x-\langle x\rangle}{2\Delta x}\right)^2 + i\frac{x\langle p\rangle}{\hbar}\right] \tag{A6}$$

and, up to an overall phase factor,

$$\langle p|\alpha\rangle = \left(\frac{1}{2\pi(\Delta p)^2}\right)^{1/4}\exp\left[-\left(\frac{p-\langle p\rangle}{2\Delta p}\right)^2 + i\frac{p\langle p\rangle}{\hbar}\right]. \tag{A7}$$

Also, the coherent states satisfy minimum uncertainty, i.e.,

$$(\Delta x)^2(\Delta p)^2 = \left(\frac{\hbar}{2}\right)^2. \tag{A8}$$

The uncertainties are given explicitly as

$$(\Delta x)^2 = \frac{1}{2a_0^2} = \frac{\hbar}{2m\omega} \tag{A9}$$

and

$$(\Delta p)^2 = \hbar^2 a_0^2/2 = \hbar m\omega/2. \tag{A10}$$

From Eq. (A4) the time evolution of these states is very simply calculated:

$$|\alpha(t)\rangle = \exp(-i\omega t/2)|\alpha \exp(-i\omega t)\rangle, \tag{A11}$$

so that

$$\langle x(t)\rangle = \langle x\rangle \cos\omega t + \frac{\langle p\rangle}{m\omega}\sin\omega t, \tag{A12}$$

$$\langle p(t)\rangle = \langle p\rangle \cos\omega t - m\omega\langle x\rangle \sin\omega t, \tag{A13}$$

where $\langle x\rangle$ and $\langle p\rangle$ are the initial expectation values of the position and momentum, respectively. Finally, the set of states $\{|\alpha\rangle\}$, where α ranges over the entire complex plane, satisfies a resolution of the identity [13]

$$\hat{\mathrm{I}} = \frac{1}{\pi}\int |\alpha\rangle\langle\alpha| d^2\alpha, \quad d^2\alpha = d[\mathrm{Re}(\alpha)] \; d[\mathrm{Im}(\alpha)]. \tag{A14}$$

The HOCSs are defined in at least three equivalent ways. As displacement operator coherent states, the coherent state is given by

$$|\alpha\rangle = \hat{D}(\alpha)|0\rangle, \tag{A15}$$

in which

$$\hat{D}(\alpha) = \exp(\alpha\hat{a}^\dagger - \alpha^*\hat{a}), \tag{A16}$$

and the operators $\hat{a}$ and $\hat{a}^\dagger$ are the usual harmonic-oscillator annihilation and creation operators, respectively. As annihilation operator coherent states, the coherent state $|\alpha\rangle$ is an eigenstate of the annihilation operator $\hat{a}$,

$$\hat{a}|\alpha\rangle = \alpha|\alpha\rangle. \tag{A17}$$

As minimum-uncertainty coherent states, since the operators $\hat{x}$ and $\hat{p}$ satisfy the commutation relation

$$[\hat{x},\hat{p}] = i\hbar, \tag{A18}$$

all states satisfy the uncertainty relation

$$(\Delta x)^2(\Delta p)^2 \geqslant \left(\frac{\hbar}{2}\right)^2. \tag{A19}$$

States that satisfy the minimum requirement in this relation (equality), i.e., the coherent states, are eigenstates of the equation [4]

$$\frac{1}{2}\left(\frac{\hat{x}}{\Delta x} + i\frac{\hat{p}}{\Delta p}\right)|\alpha\rangle = \alpha|\alpha\rangle, \qquad \alpha = \frac{1}{2}\left(\frac{\langle x\rangle}{\Delta x} + i\frac{\langle p\rangle}{\Delta p}\right). \tag{A20}$$

This alone defines a broader set of states than the coherent states. Imposing the two conditions (A8) and that $|\alpha=0\rangle = |n=0\rangle$ [cf. Eq. (A2)] restricts this set to that of the coherent states themselves.

[1] E. Schrödinger, Naturwissenschaften **14**, 664 (1926) [*Collected Papers on Wave Mechanics*, 3rd ed. (Chelsea, New York, 1982)].

[2] I. Zlatev, W.-M. Zhang, and D. H. Feng, Phys. Rev. A **50**, R1973 (1994).

[3] J. R. Klauder, J. Phys. A **29**, L293 (1996).

[4] M. M. Nieto and L. M. Simmons, Jr., Phys. Rev. D **20**, 1321 (1979).

[5] M. M. Nieto and L. M. Simmons, Jr., Phys. Rev. D **20**, 1332 (1979).

[6] M. M. Nieto and L. M. Simmons, Jr., Phys. Rev. D **20**, 1342 (1979).

[7] M. M. Nieto, Phys. Rev. D **22**, 391 (1980).

[8] V. P. Gutschick and M. M. Nieto, Phys. Rev. D **22**, 403 (1980).

[9] M. M. Nieto, L. M. Simmons, Jr., and V. P. Gutschick, Phys. Rev. D **23**, 927 (1981).

[10] *Coherent States: Applications in Physics and Mathematical Physics*, edited by J. R. Klauder and B.-S. Skagerstam (World Scientific, Singapore, 1985).

[11] S. Flügge, *Practical Quantum Mechanics* (Springer-Verlag, Berlin, 1971).

[12] I. S. Gradshteyn and I. M. Ryzhik, *Table of Integrals, Series and Products*, 4th ed. (Academic, New York, 1965).

[13] C. Cohen-Tannoudji, B. Dui, and F. Laloë, *Quantum Mechanics* (Wiley, New York, 1977), Vols. 1 and 2.

[14] K. Bhaumik and B. Dutta-Roy, J. Math. Phys. **16**, 1131 (1974).

[15] P. M. Benoit, S. M. McRae, and E. R. Vrscay, in *Quantum Dynamics of Chaotic Systems*, Proceedings of the Third Drexel Symposium on Quantum Nonintegrability, edited by J. Yuan, D. H. Feng, and G. M. Zaslavsky (Gordon and Breach Science, Langhorne, PA, 1993).

[16] S. M. McRae and E. R. Vrscay, J. Math. Phys. **38**, 2899 (1997).

[17] L. E. Ballentine, Y. Yand, and J. P. Zibin, Phys. Rev. A **50**, 2854 (1994).